

Proc. of CMM Technical Conf. on  
Ocean Waves. WMO/TD No. 350, Report 24  
1990.

LOCAL AND REGIONAL SCALE WAVE MODELS\*

by

DESIRAJU B. RAO

NATIONAL METEOROLOGICAL CENTER

WASHINGTON, D.C., 20233 U.S.A.

ABSTRACT

*The development of regional and local scale ocean wave forecast models at the National Meteorological Center (NMC) is discussed. Some results from a second generation shallow water spectral wave forecast model implemented on the Gulf of Mexico and a local wave forecast model developed for the entrance of the Columbia River using ray tracing technique are presented.*

I. Introduction:

The methods employed to forecast ocean waves were originally based on empirical techniques developed by Sverdrup and Munk and subsequently modified by others (see Hubert, 1964 for a review). These methods provide information on significant wave heights due to swell and local wind sea. Even though these empirical techniques are still being used to forecast (and hindcast) waves for special situations both at NMC and elsewhere around the world, it has become clear that further advances in our understanding of wave processes (such as growth, propagation, dissipation, and non-linear energy transport) and our ability to improve the wave forecasts requires a different approach. The state of wave forecasting has now gone through significant advances with the recognition that in reality the sea surface can, and should, only be described as a random superposition of several wave components. Hence only the statistical properties of the motion should be viewed as either observationally significant or theoretically predictable. This concept led to the introduction of the wave spectrum and the formulation of the time-dependent spectral wave energy balance equation. In its simplest form, the growth (or decay) of the spectral wave energy density  $F(f, \theta)$  -  $f$  is the frequency and  $\theta$  is the direction- at any point is determined by the advection of energy by the group velocity, energy input from the winds at the ocean surface, dissipation of energy due to various sources, and non-linear interactions between the wave components (for example, see Phillips, 1980, for a review of wave dynamics). In this approach, the significant wave height is simply proportional to the square root of the energy over all frequencies and directions.

Parallel with the theoretical development of the spectral wave forecasting techniques, the demands for spectral wave information also have been increasing for various applications. However the forecasting of waves using the spectral method in its most general form requires considerable computational resources. The most time consuming part of the spectral energy equation is the calculation of the non-linear wave interactions (which redistribute the energy among the various frequencies and thereby determine the spectral shape but do not change the total energy under the spectrum). Hence a hierarchy of spectral

---

\*OPC publication No. 35



wave forecast models has evolved to optimize the computer time. These models are commonly referred to as the first, second, and third generation models– 1G, 2G, and 3G. In the 1G models, the non-linear terms are completely suppressed, in the 2G models they are calculated by approximate (parameterized) representations, and in the 3G models an attempt is made to calculate them more exactly (see the SWAMP group report, 1985).

The NMC routinely provides ocean wave guidance forecasts on global, regional, and local scales to the weather service forecast offices with marine responsibilities. For the purposes of this article, a regional scale is defined as one that spans a limited area (less than global) and a local scale is considered to be one that is applied to a specific site. Even though there are still a few forecasts issued for selected locations by NMC using the empirical techniques, a systematic effort has been initiated to replace all forecasts based on spectral approach. A 2G deep water global model has been operational for over three years and a regional shallow water 2G model has become operational over the Gulf of Mexico in the last year. The regional model is now being modified to cover the Gulf of Alaska and the continental shelves along the east and west coasts of the U.S. At the same time, efforts are underway to develop site specific forecasts using ray tracing techniques to bring the wave spectrum from either the global or a regional model to selected locations. This article presents a brief review of the techniques developed to provide the guidance for the regional and local areas.

## II. Regional Scale Model:

Even though the operational global wave models of NOAA (NOW) and the U.S. Navy (GSOWM) have grid points along the continental shelves and the gulfs adjacent to the U.S coast line at which forecasts are available, these forecasts are not capable of representing the true wave conditions over these areas for reasons mentioned below. These global scale wave models are deep water models with coarse horizontal resolution to economize the computer time. The large grid spacing precludes a reasonable resolution of the geometry of the region– such as the presence of any islands and barriers– and mesoscale features of the ocean surface winds. Since most regional models are likely to be in coastal areas or gulfs, the water depth in the region would range from shallow to intermediate values. Refraction and shoaling by bathymetry, as well as diffraction around islands and structures, may be substantial. Dissipation of wave energy by bottom friction also becomes important in shallow water. This process depends on the details of the wave induced flow in the bottom boundary layer and the composition of the bottom material, and is not an easy process to represent accurately. In regions dominated by strong oceanic currents, complicated wave–current interactions result in significant modifications of the wave spectrum. In a regional domain, mesoscale variations in the wind field play an important role in determining the sea state. All of these factors are absent in a global scale model and these, also, are the factors that contribute to the errors in wave forecasts in any regional model. Another complication in regional modeling is having to prescribe the deep ocean wave conditions along open boundaries across which wave trains propagate into the domain of interest; thus making any regional model susceptible to boundary errors which are normally obtained from a larger (global) scale model.

### (a) Model description–

In order to isolate the performance characteristics of the regional model by itself, the model developed at NMC for regional applications was first implemented on the Gulf of Mexico because, for all practical purposes, it is a closed basin with very little wave energy transfer between the Gulf and the open ocean. This model is essentially based on the one developed by Golding (1983) for operational use by the British Meteorological Office. The model solves the energy balance equation:



$$\frac{\partial F}{\partial t} = -\nabla \cdot \vec{C}_g F - \frac{\partial \left[ \left( \vec{C}_g \cdot \nabla \theta \right) F \right]}{\partial \theta} + I + D + N \quad (1)$$

$$2\pi f = \sqrt{gk \tanh kh}; \quad k = \sqrt{k_x^2 + k_y^2} = |\vec{k}|$$

$$\vec{C}_g = \pi \frac{f}{k} \left\{ 1 + \frac{2kh}{sh2kh} \right\} \frac{\vec{k}}{k} \quad (\text{group velocity vector})$$

In the above equation,  $t$  is the time,  $\nabla$  is the horizontal gradient operator,  $F(f, \theta)$  is the spectral density of the wave of frequency  $f$  (in Hz) propagating in the direction  $\theta$ , and  $H$  is the water depth.  $k_x$  and  $k_y$  are the  $x$  and  $y$  components of the wave number vector and their values change as  $\theta$  and  $H$  change in such a way as to conserve the value of the frequency  $f$ .

The first term on the right hand side of Eq. (1) represents the propagation of wave energy by the group velocity from one point to another and the second represents the refraction of the wave train by changing bottom topography. The effect of bottom topography ( $h$ ) is explicitly contained in the expressions for the frequency and the group velocity. In a deep water model the frequency is independent of depth. Hence, group velocity does not contain the depth factor and the second term is absent.  $I$  is the energy input into the ocean from the winds which are responsible for generating the waves,  $D$  is the dissipation of wave energy, and  $N$  represents nonlinear interactions between the waves. The latter process is an energy conserving process which governs the shape of the wave spectrum.

The energy balance equation is solved numerically in a sequential manner— propagation, refraction, growth and dissipation, and nonlinear interactions— just as given on the right side of Eq. (1). For the sake of brevity, the numerical schemes and the representation of the various processes used in solving the equation are described only in a qualitative manner in order to provide a basic understanding of the mechanics involved in developing a wave forecast model. However, the references necessary to obtain the details are cited in the text.

The computation of wave propagation is based on a higher order finite difference scheme than the one used by Golding in order to reduce numerical dissipation and dispersion. This scheme is described in Duffy and Atlas (1984) in their study of the wave conditions generated by the QE II storm in the Atlantic in 1978. The wave refraction calculation in shoaling water is the same as Golding's scheme. The wave growth by winds is computed using the conventional linear (Phillips growth) mechanism representing the wave excitation by the turbulence fluctuations in the wind field and the exponential (Miles) mechanism representing energy transfer to the waves by the wind shear in the boundary layer flow above the ocean surface.

The inclusion of the dissipation term in the energy balance equation ensures that the wave spectrum is limited by the Pierson –Moskowitz (P–M) spectrum (see Pierson and Moskowitz, 1964) as the wave growth approaches a state of full development. The processes for wave energy dissipation taken into account here are whitecapping, bottom friction, and percolation. The dominance of a dissipation process is determined by the ratio of the local depth of the water column to the wavelength. In deep water (depth  $>$  half the wavelength), the dissipation is attributed to whitecapping. This process involves the entire wave spectrum and is prescribed according to the procedure used by Golding based on the work of Hasselmann (1974). In shallow water (depth  $<$  half the wavelength), the dissipation is primarily due to bottom friction and percolation. The loss due to bottom friction is treated the same way as Golding who used a represen-



tation proposed by Collins (1972). The dissipation due to percolation depends on the geological properties of the bottom material and the method proposed by Shemdin et al (1980) was used in the model.

As mentioned earlier, an exact treatment of the nonlinear interaction terms requires a substantial computational effort. To avoid this, they are treated in a parameterized form. The first step in the process is the introduction of the concept of a "wind sea spectrum". To obtain the wind sea spectrum, the peak energy frequency  $f_p$  of the P-M spectrum corresponding to the prevailing wind speed at that instant is determined. Then the energy densities in all those directional-frequency bands with frequencies  $f > 0.8 f_p$  and directions lying within  $\theta_w - 90 < \theta < \theta_w + 90$ , where  $\theta_w$  is the prevailing wind direction, are integrated to obtain the total energy in the wind sea. Since the P-M spectrum is considered to be valid only for an equilibrium state, the peak frequency  $f_p$  given by that spectrum would not correspond to the true peak frequency in a wave spectrum that is evolving in time under the influence of the local winds and nonlinear interactions. Since the nonlinear interactions do not change the total energy, an iterative calculation is done in which the computed total wind sea energy and the estimate of  $f_p$  from the P-M spectrum are used to calculate a new peak frequency based on considerations presented by Hasselmann et al (1976). This new estimate of the peak frequency and the total wind sea energy are then used to construct a JONSWAP spectrum so that the energy is conserved. The spectral energy distribution resulting from this synthesized JONSWAP spectrum is used to replace all the computed energy densities in the "wind sea spectrum" using a cosine-squared law for directional distribution. The rationale behind this apparently artificial manipulation is the belief that the nonlinear interactions between the waves will always force the shape of the wind sea spectrum to correspond to the shape of the JONSWAP spectrum. Since the nonlinear interactions do not change the total energy, this energy conserving manipulation presumably mimics the final result of a more exact calculation with considerably less computational effort. In shallow water the basis for constructing the equivalent JONSWAP spectrum is modified from the deep water case to reflect the fact that the waves steepen more rapidly under stronger nonlinear interactions. Hence a modified JONSWAP spectrum is defined that forces the wind sea spectrum to conform to the saturation range in water of arbitrary depth (Thornton, 1977).

#### (b) Wind field specification-

The most important step in generating and forecasting waves is the specification of the wind field in the boundary layer over the ocean surface. For the Gulf of Mexico, the forecast winds are obtained from the operational regional nested grid model of NMC (see Hoke, 1984). This is a grid point model covering the northern hemisphere with three nested grids. The outermost grid has a grid resolution of approximately 320 km, the next inner grid has a 160 km resolution, and the innermost grid, which encompasses the area covering the U.S. (including Gulf of Mexico), has a 80 km resolution in the horizontal direction. The vertical coordinate in the model is a sigma coordinate and the lowest sigma layer has a thickness of 35 mb. Since the winds are computed in the numerical model at the mid-point of the layer, they are available at a height of approximately 175 m above the sea level. Since this level is above the constant flux layer, a diagnostic boundary layer model developed by Cardone (1969) is used to reduce the winds to a 10 m height above the ocean. The Cardone model takes into account the effects of the Ekman boundary layer and the constant flux layer in deducing the 10 m level winds from the large scale weather prediction model's output fields. The Cardone model also allows for corrections due to stability effects produced by air-sea temperature differences.

#### (c) Results-

A grid interval of approximately 55 km in the east-west and north-south direction is used to represent the Gulf of Mexico domain, resulting in a total of 37x27 grid points (Figure 1). The Gulf is closed along the Yucatan Strait and the Straits of Florida. Since these straits are narrow and the observed swell in the straits is not well developed, it can be assumed that the local wave conditions in the Gulf are not much



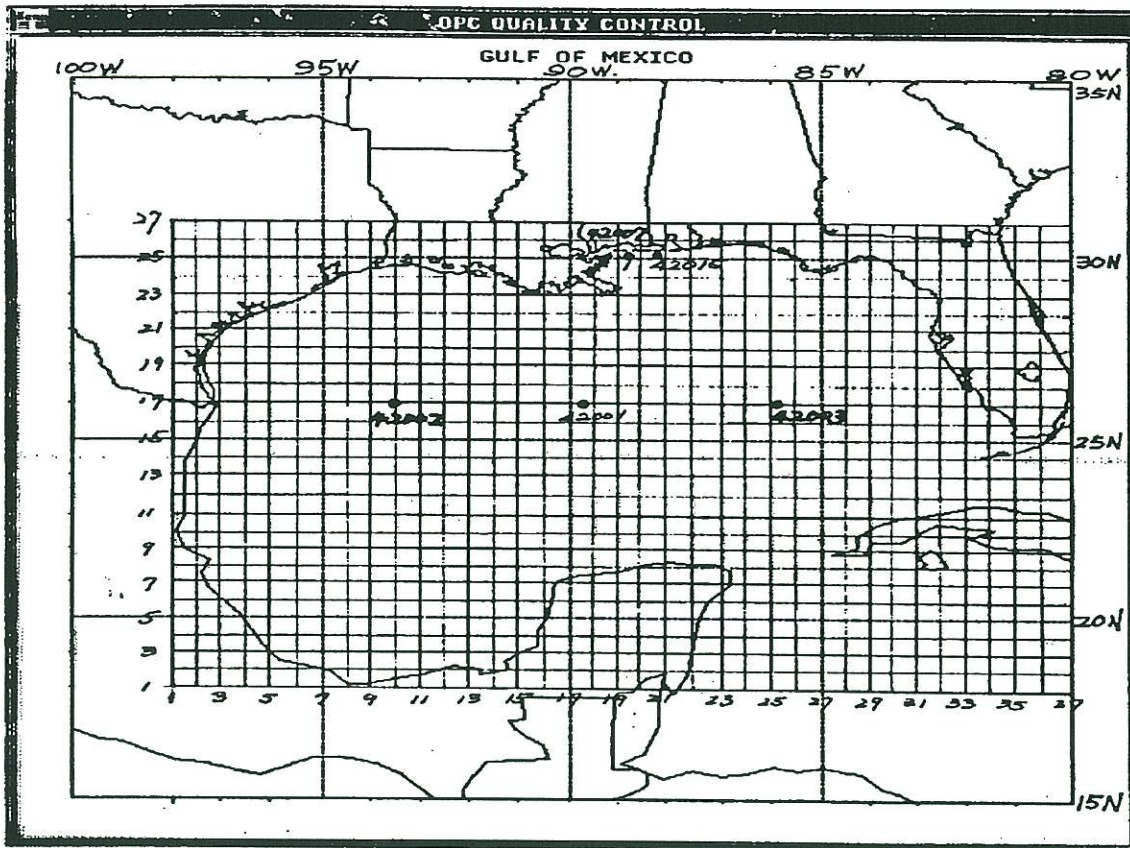


Figure 1. Gulf of Mexico grid. Locations of buoys are also shown.

influenced by conditions in the open ocean. This permits an assessment of the performance of the model forecasts without the complication of errors introduced by the boundary conditions at the open boundaries. The model has twenty equally spaced frequency bands ranging from 0.04 to 0.42 Hz and twelve directional bands, thus providing 240 degrees of freedom to represent the two-dimensional wave spectrum at each point. The time step used for forecasting is 30 minutes. The forecasts are issued on the 00 and 12 UTC cycles and extend to 48 hours. The guidance forecasts are issued to the field forecast offices in 12 hour intervals in the form of contours of significant wave heights and arrows to show the direction of propagation of the primary wave (the maximum energy frequency wave).

The model was run on a test basis for several months before operational implementation in September 1988. During the test phase, as well as after the implementation, the model forecasts are compared to wave measurements from buoys deployed in the Gulf of Mexico by the National Data Buoy Center of NOAA. The comparisons have been mostly carried out in terms of the significant wave heights predicted by the model (and interpolated to the buoy location) and those measured by the buoy at the corresponding valid times. Statistics used for the evaluation are the conventional definitions of bias, root mean square error (RMS), and correlation coefficient.

Figure 2 shows these statistics for 24 hour forecasts during October 1987 to February 1989 at a deep water buoy (42001) located in the center of the Gulf. In this figure, statistics calculated for the forecasts from the new regional model (GMEX) are shown, as well as those from the global deep water models of the Navy (GSOWM) and NOAA (NOW). It is clear that during the testing period (prior to September 1988), the regional model showed a consistently better performance than the global models when the RMS and the correlation coefficients are considered. It showed a negative bias in the early stages of the testing period, but this bias was being gradually reduced at the time of implementation. However, immediately after operational implementation, the regional model appears to have suffered a set back, particularly in the RMS error when compared to the global models. This was due to the rather active hurricane season that the Gulf region experienced in the fall of 1988 in contrast to the fall of 1987 when the model testing was started. The boundary layer algorithm that derives the winds from the regional weather prediction model is based on geostrophic and Ekman considerations and, hence, was not designed to handle hurri-

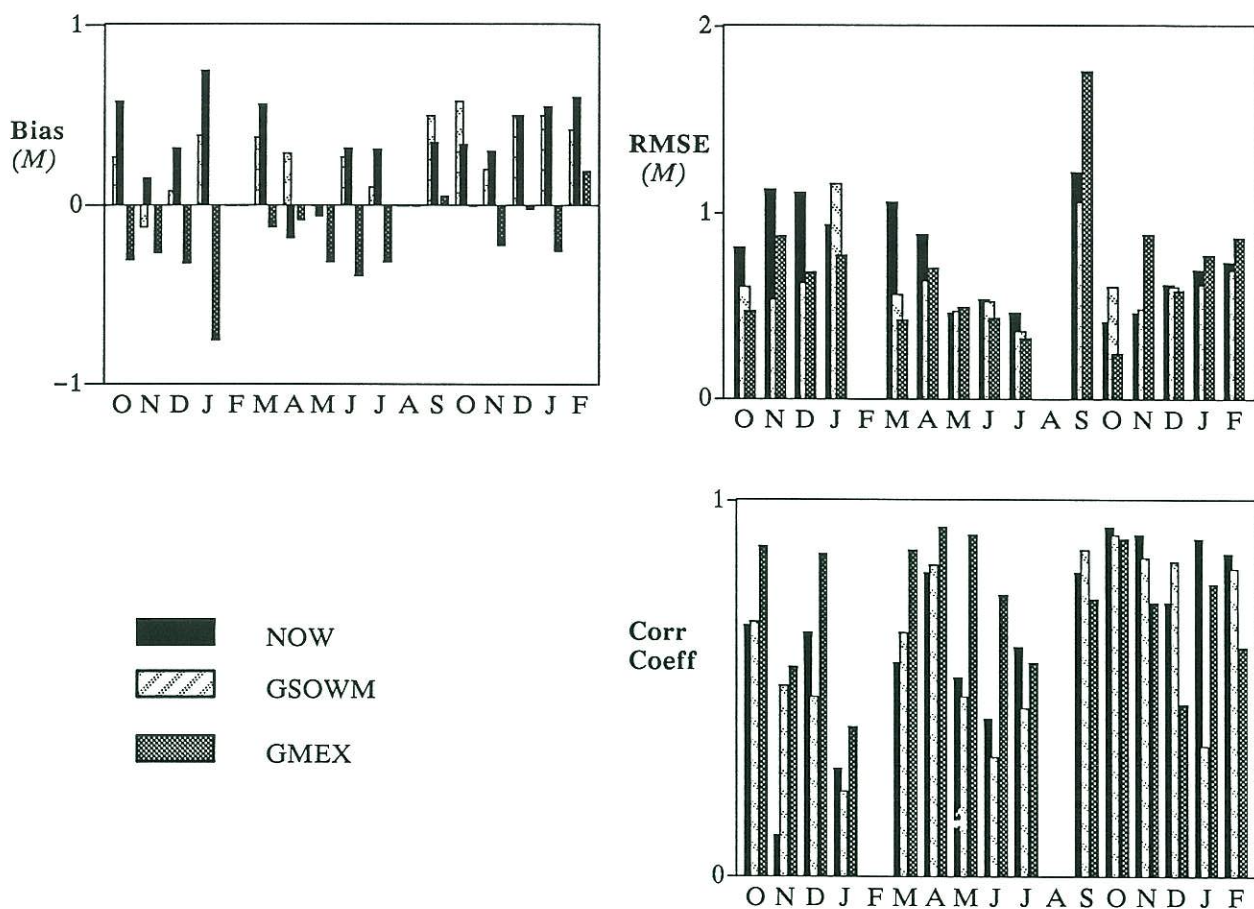


Figure 2. Error statistics for 24-hour forecasts from the regional and global forecast models at the location of deep water buoy 42001. The period cover is from October 1987 to February 1989.



cane type situations. Consequently, the wind forecasts provided to the wave model were seriously in error, which in turn degraded the quality of the wave forecasts. On the other hand the global wave models of the Navy and NOAA use different boundary layer algorithms to deduce the winds from global scale weather prediction models and were not as much affected by the hurricanes as the regional model. It is clear from this experience that the wind input to the model is a critical source of error. The problem of deriving better wind fields in the marine boundary layer, particularly in hurricane situations, is being currently examined.

Figure 3 shows the error statistics for a shallow water buoy (42015) located in a water depth of 16 m. At this buoy, the statistics from the global models are not presented since the water depth is very shallow. It shows that the monthly mean bias and the RMS errors are very small. The correlation coefficient appears to be satisfactory for the most part but efforts are being made to further improve it by tuning the bottom friction and percolation parameterizations in the model.

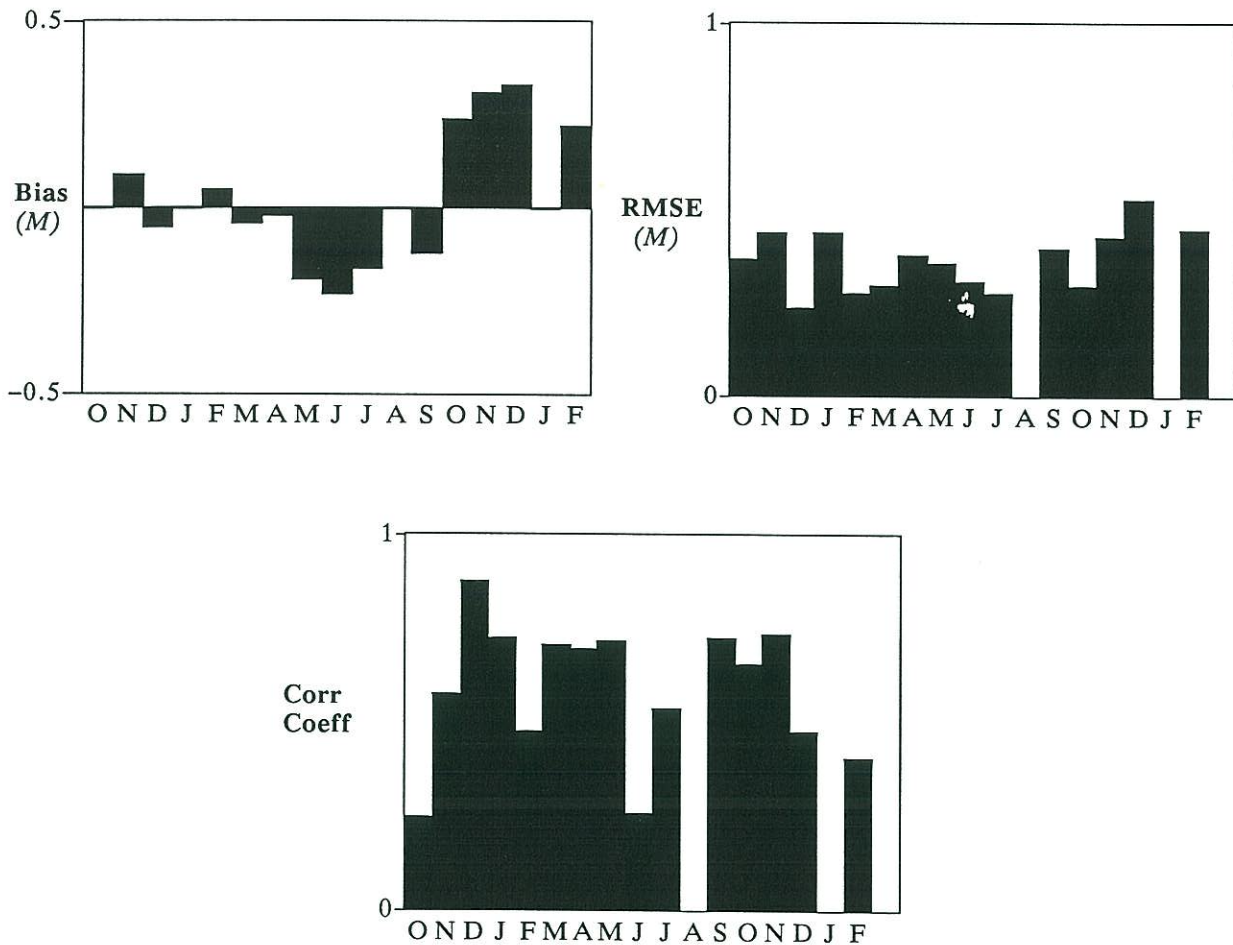


Figure 3. Error statistics for 24-hour forecast from the regional model at the location of the shallow water buoy 42015. The period covered is from October 1987 to February 1989.

### III. Local scale model:

There are certain locations, particularly on the west coast and the Alaskan coast of the U.S., where local currents are intense and where there are major bottom topographic features that act together (or individually) to significantly modify the open ocean wave trains propagating into the location. The interaction between the incoming waves, currents, and bathymetry often produce wave conditions that are hazardous to shipping, particularly during times of ebb currents.

In order to provide guidance for these locations, a ray tracing technique is employed in which the deep water spectrum is brought to the location, taking into account the effects of currents and two-dimensional bathymetry. The entrance to Columbia River on the west coast of U.S. was chosen as the site to develop the program initially. This location is characterized by strong currents produced by the tidal regime and river outflow, bathymetry which is dominated by the presence of bars at the entrance to the river, and a location usually subject to the incidence of large swells from the Pacific Ocean. All these factors contribute to the creation of hazardous conditions for shipping resulting in numerous accidents and occasional loss of life.

#### (a) Model description-

As in the case of the discussion on the regional model, only a brief description of the underlying concepts in a ray tracing method is presented here. The reader is referred to Lighthill (1978) for a general theory of ray tracing and to Peregrine (1976) for a treatment of various wave-current interaction problems. A complete description of the model for the Columbia River entrance is presented in Chao and Bertucci (1989).

As the spectral energy components  $(f, \theta)$  of a two dimensional wave spectrum propagate towards a coast from the open ocean, the path followed by each frequency-directional component is called a ray. The path of each ray between the open ocean, and the coast and the time taken to reach the coast, are influenced not only by its  $f$  and  $\theta$  values at the point of origin, but also by the orientation of the coast line, changes in bottom topography, and the presence of any significant ocean currents in the intervening area. The frequency changes along the ray, to say  $f'$  (called the intrinsic frequency), from its original value  $f$  (called the apparent frequency) due to ocean currents (Doppler shift) and changes in bottom topography. Using the notation of Eq. (1),  $f'$  is given by:

$$2\pi f' = \sqrt{gk' \tanh k'h} = 2\pi f - \vec{U}' \cdot \vec{K}' \quad (2)$$

$$\vec{U}' = \text{ocean current vector}$$

Given the ocean current vector, local depth  $h$ , and the apparent frequency  $f$ , the above equation can be solved to determine  $k'$  and the angle of travel  $\theta'$  using kinematic principles (eg. see Phillips, 1980); and hence  $f'$ . The wave number  $k'$  and the direction of travel  $\theta'$  change along the ray under the combined influence of depth variations and currents (refraction). Hence, not only the time it takes for a spectral component to travel along its ray from a source point to a point where it ultimately impinges on the coast changes from one spectral component to another, but also the location where each component impinges on the coast changes. In addition, even for the same spectral component from a given source point the travel time along its ray and the ray path, which determines its point of impingement on the coast, also change during different current regimes such as the high and low tide periods. Finally, it should be noted that the value of the spectral energy density  $F(f, \theta)$  also changes along each ray to some  $F'(f, \theta')$  by the time the ray reaches the coast.



It might appear, a priori, from the above discussion that the ray tracing technique may not be a convenient tool to use for forecasting waves at a coastal- or target - point. However, a certain dynamical property, which is conserved along each ray, makes it feasible to adopt the technique for forecasting waves at a target location from information provided in the source region. As shown by Bretherton and Garrett (1969), the “wave action” –defined as the ratio of the wave energy density  $F'(k_x', k_y')$  divided by the intrinsic frequency  $f'$  – is a constant along each ray as wave trains move from a source to a target point through an inhomogeneous medium, such as one characterized by changing bottom topography and variable ocean currents. The energy density expressed in terms of the wave numbers can be related to the energy density in terms of frequency and direction through the use of the frequency equation. In terms of the frequency–directional spectrum, the conservation property can be stated as:

$$\frac{c'_g + U' \cos \theta' + V' \sin \theta'}{k'} \frac{F'(f, \theta')}{f} = \text{constant along a ray} \quad (3)$$

It is this property that permits the calculation of the change in the spectral energy density as the wave spectral components propagate from any source location to their respective destinations at the coast.

Consider now the problem of developing a forecasting scheme based on ray tracing techniques for a target point on the coast using available information on the wave spectrum (either measurements or forecasts) at some source points in the deep water. At any given instant, the wave spectrum at the forecast point is determined by the energy densities transported to the point by the waves arriving there simultaneously from the contributing source points along each of their own ray paths. In practice, it is a rather difficult problem to deduce a priori, particularly when different ocean current regimes have to be considered, which rays from the source points would contribute to the local sea at the forecast time. Hence, a scheme was designed by Dorrestein (1960) to trace the rays in the reverse direction from the target point to the open ocean region where the source point (s) are located. For this, the azimuthal domain at the target point over which waves are likely to arrive from the open ocean is divided into a number of directional sectors– given by  $\theta'$ . Since the frequency components  $f$  at which wave spectral information is available in the source region is known, rays and travel times are calculated for direction–frequency components designated by  $f$ – $\theta'$  from the target point to the source region. Each of the  $f$ – $\theta'$  components would terminate in the source region after different travel times and at different locations (X,Y) determined by the ray paths. Normally, neither the terminal point nor the angle  $\theta$  at which each ray arrived at its terminal point would coincide with an available measurement or forecast point in the source region. However, since the observation or forecast points in the source region are set up to provide wave information continuously at selected time intervals, it is an easy matter to interpolate to the location (X,Y) and the appropriate time of arrival of each ray to obtain the spectral energy density  $F(f, \theta)$  corresponding to the frequency  $f$  and the angle of arrival  $\theta$  at the source point. These rays and the travel times can then be computed for any target point over a range of expected variations in the ocean currents over the domain and a scheme can be set up to obtain the required values of  $F(f, \theta)$  that are needed to issue a wave forecast at the target point at a given time . Also, if the coefficient multiplying the  $F'(f, \theta')$  in Eq. (3) at the target location is designated by  $A'(f, \theta')$ , and the corresponding value of it at the source location (X,Y) is  $A(f, \theta)$ , then the spectral energy density at the target is given by:



$$F'(f, \theta') = \frac{A(f, \theta)}{A'(f, \theta')} F(f, \theta) \quad (4)$$

The values of A and A' for all of the required spectral components can be computed once for all from the kinematic considerations mentioned earlier. The ratio A/A' is called the amplification factor. Hence, once the spectral density at the source point (X,Y) is obtained from interpolation using the measurement or forecast points in the source region, the spectral densities in all f-θ' components at the forecast point are known, and the significant wave height can be computed by the usual procedure.

Some of the limitations of the above method are that no provisions are made for generation of wind seas by local winds (which sometimes can be significant ) and for dissipation of wave energy by bottom friction. Since waves are likely to steepen and grow when a wave train is propagating against the ambient current, allowance is made to prevent the growth of the spectral energy density from reaching unrealistically large values. This is done by assuming the Wallop's spectrum (Huang et al, 1983) for finite depth as the limiting spectrum. Whenever the computed energy density exceeds that of the Wallop's spectrum, it is set equal to the value given by the Wallop's spectrum.

(b) Results-

Figures 4 and 5 show the amplification factors for an ideal linearly sloping bottom and for the actual two-dimensional bottom topography at the Columbia River entrance region for three different current regimes. The current regimes considered are - current of 3 m/s towards the coast (+ sign) and away from the coast (- sign), and no current. The amplification factors in each panel are given as function of the incidence angle θ' at the forecast point for three frequency components. In both the one and two dimensional cases, it is clear that the amplification factors change significantly when the current is directed away from the coast and, hence, opposing the incoming waves. It is also clear that in this case the amplification factors from the one and two dimensional considerations differ significantly in their magnitudes. In computing the amplification factors for the two-dimensional case, the domain taken into account is encompassed between longitudes 125.0 and 124.1 degrees west and latitudes 45.0 and 47.5 degrees north. The mouth of the river is located at 124.1 west and 46.2 north. A grid resolution of 5 n mi was used in the computations.

The Seattle forecast office issues routine wave forecasts for the entrance of the Columbia River using a combination of the wave conditions reported by a buoy located in deep water at some distance from the river mouth (and hence not representative of the local conditions), and a one-dimensional model developed by Gonzalez (1984) with an idealized linearly sloping bottom topography. The forecasts are issued in terms of the expected high and low values (range) of the wave heights. Fig.6 shows a time sequence of forecasts issued by the forecast office (only the high values are plotted in the figure) and those calculated from the present two-dimensional model. For the two-dimensional model, the spectral densities in the open ocean region that are needed to compute the significant wave height at the river entrance are taken from two forecast points from the operational deep water global wave model (NOW). These points are located at 125.0 W, 45.0 N and 125.0 W ,47.5 N. It is clear that sometimes there are large differences between these two forecasts. This is a consequence of the fact that the amplification factors for the one and two dimensional cases differ as was shown in Figs. 4 and 5. Unfortunately, the environment at the entrance to the river is too harsh to maintain a wave measurement system over any extended period of time due to the prevailing wave conditions and strong currents. Hence, adequate data taken at the mouth of the river are not available to make a systematic assessment of the forecasts issued by the forecast office



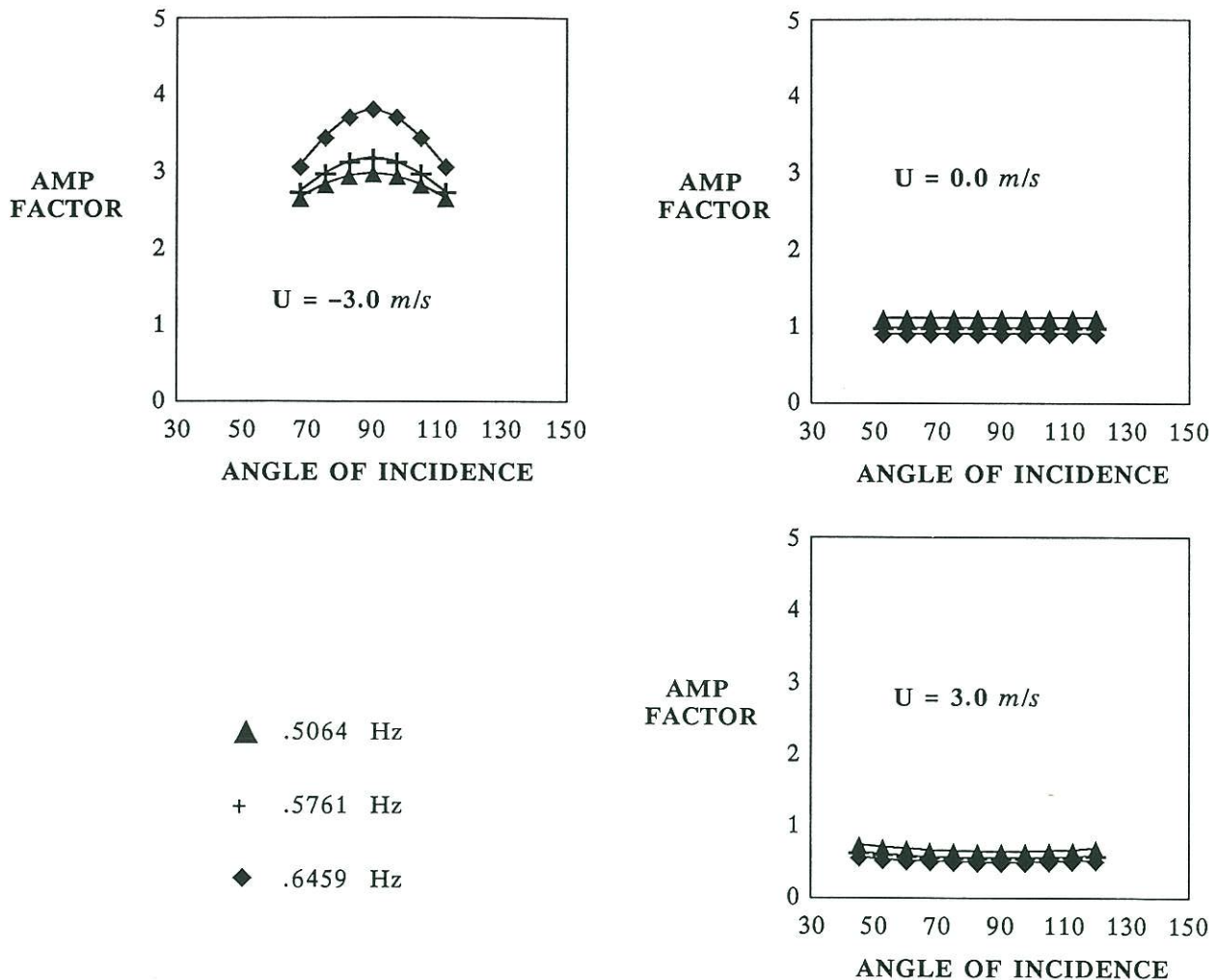


Figure 4. Amplification factors for three different frequencies as a function of the angle at the forecast point for a linearly sloping bottom. Each panel shows the amplification factors for different ocean current regimes.

and those produced by this model. The fact that there are sometimes significant differences between the two forecast points out the immediate necessity to carry out any verification, however qualitative, that could possibly be done under the circumstances. Efforts are underway to make at least a temporary arrangement to gather some measurements to accomplish this purpose.

A simple operating procedure using ray tracing method can be set up so that an individual forecast office can produce their own local forecast on a personal computer (PC) using the deep water wave forecast guidance received from NMC. A program can be provided on a floppy disc containing the table of amplification factors, travel times and the locations (X,Y) of the terminal points, and the space-time interpolation scheme to obtain the spectral densities in the source region for each expected ocean current regime. The inputs to the program are the expected speeds of the local currents at the forecast time (prescribed by the forecast office) and the wave spectral energy densities at the deep water points (provided by NMC over the communications link). The program then obtains the  $F(f,\theta)$ 's in the source region using the interpolation scheme and multiplies them by the appropriate amplification factors to produce a local

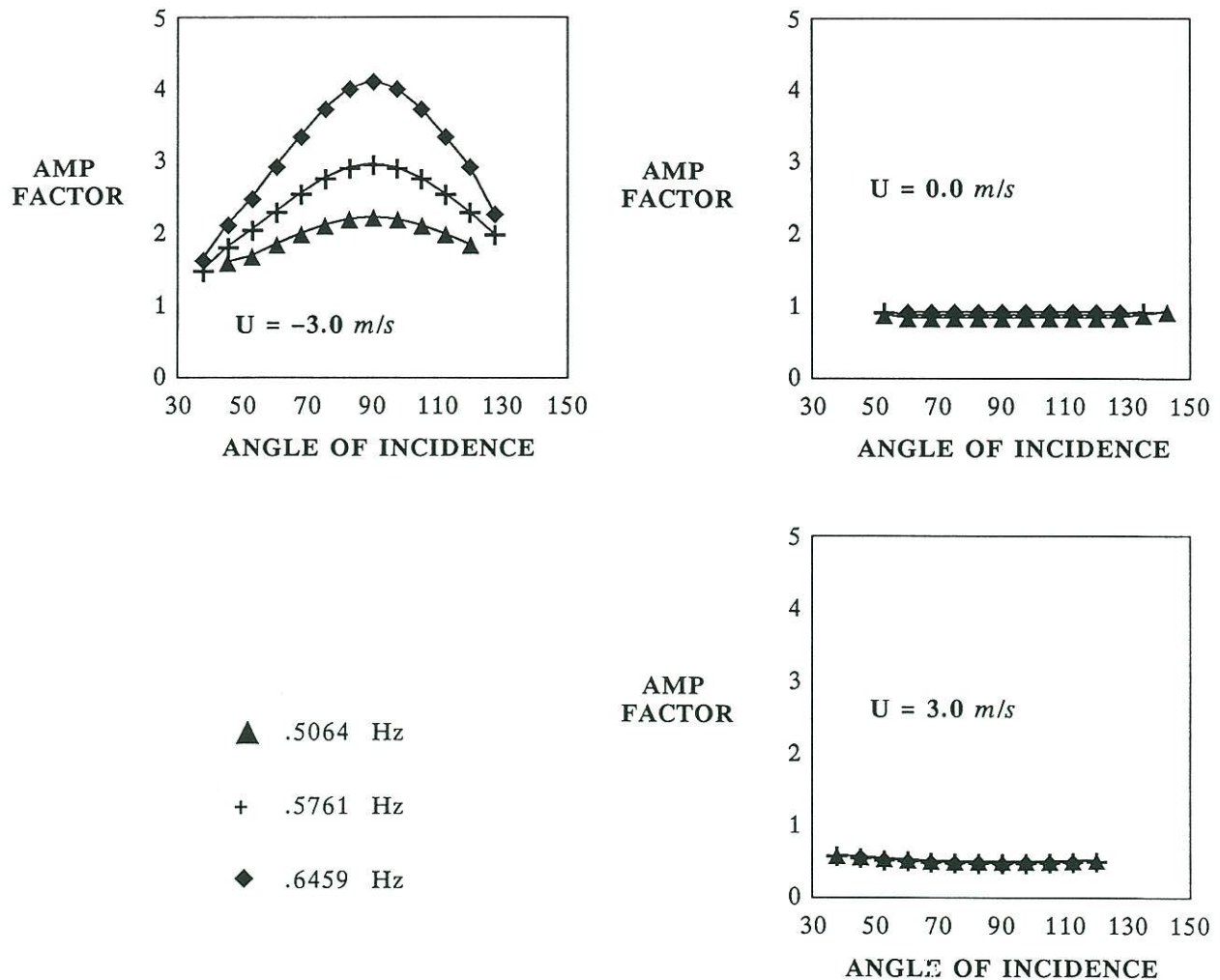


Figure 5. Amplification factors for three different frequencies as a function of the angle at the forecast point for the actual two dimensional topography off the entrance to the Columbia River.

forecast. The major sources of errors in the forecasts are the spectral energy densities provided by the global forecast model in the source region and the prescription of the currents. Efforts to improve the performance of the global wave forecast model are continuing at NMC, and the contribution to local forecast errors through this source should be minimized in the near future. The problem of specifying the ocean currents and river outflow at the mouth is, however, a formidable problem. Since a central guidance facility, such as NMC, is not in a position to specify with any accuracy the conditions of the local currents at a forecast point, a PC based program provided to the forecast office allows them to use their own judgment about the most appropriate current regime to use in producing a final forecast. Such a program has been developed and will be tested shortly with the cooperation of the Seattle forecast office. This type of modeling approach is now being applied to other locations starting with selected points on the Alaskan coast.



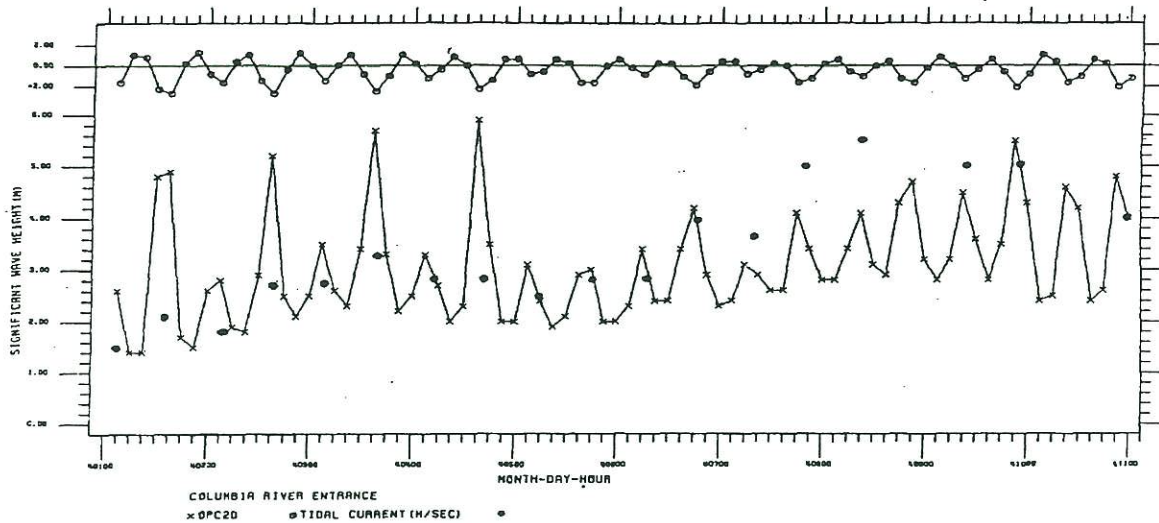


Figure 6. Wave height forecasts produced by the two-dimensional model, solid trace. The dots are the highest wave heights actually forecasted by the forecast office. The curve at the top of the diagram shows the tidal currents (in  $m/s$ ) prescribed at the mouth of the Columbia River.

#### IV. Summary:

Waves generated in the open ocean and propagating into specific regions and locations undergo significant modifications due to, for example, changes in the geometry of the domain, changes in the bottom topography, effects of bottom friction, mesoscale changes in the wind field, and the presence of dominant ocean currents. These effects cannot be resolved in a global scale wave forecast model since they occur on a spatial resolution which is much less than the grid resolution of the global models, and also since some of the processes are not included in the global models. Hence, there is a need to consider the development of regional and local scale models which can take into account important aspects that come into play to modify the incoming wave trains and use them to produce forecasts with the outer boundary conditions provided by the global models.

The basic principles involved in the development of a second generation spectral wave model for regional wave forecasting and a ray tracing approach to local wave forecasting have been discussed. Some results on the performance of the regional Gulf of Mexico model are shown using data from the buoys deployed in the Gulf. Local forecasts generated for the entrance of the Columbia River have also been discussed.

#### V. Acknowledgments:

I am grateful to Y.Y Chao for several discussions on the content of the paper and to Tina Bertucci for help with the drafting of figures. The editorial assistance of Dave Feit is also very much appreciated.

#### REFERENCES

- Bretherton, F.P., and C.J.R. Garrett, 1969: Wavetrains in inhomogeneous moving media. Proc. Roy. Soc. A, 302, 529-554.
- Chao, Y.Y., and T. Bertucci: 1989: A Columbia River entrance wave forecasting program developed at the Ocean Products Center. OPC Tech. Note No.33.

- Cardone, V.J., 1969: Specification of the wind field distribution in the marine boundary layer for wave forecasting. Report TR-69-1, Geophys. Sci. Lab., New York Univ.
- Collins, J.I., 1972: Prediction of shallow water spectra. *J. Geophys. Res.*, 77, 2693-2707.
- Dorrestein, R., 1960: Simplified method of determining refraction coefficients for sea waves. *J. Geophys. Res.*, 65, 637-642.
- Duffy, D.G., and R. Atlas, 1984: Surface wind and wave height prediction for the QEII storm using SEASAT scatterometer data. *Proc. of Oceans '84 Conf., Marine Tech. Soc.*, 183-188.
- Golding, B.W., 1983: A wave prediction system for real time sea state forecasting. *Quarterly J. Roy. Met. Soc.*, 109, 393-416.
- Gonzalez, F.I., 1984: A case study of wave-current-bathymetry interactions at the Columbia River entrance. *J. Physical Oceanog.*, 14, 1065-1078.
- Hasselmann, K., 1974: On the spectral dissipation of ocean waves due to whitecapping. *Boundary Layer Met.*, 6, 107-127.
- Hasselmann, K., D.B. Ross, P. Muller, and W. Sell, 1976: A parametric wave prediction model. *J. Physical Oceanog.*, 6, 201-228.
- Hoke, J.E., 1984: Forecast results from NMC's new regional analysis and forecast system. 10th. AMS Conf. on Weather Forecasting and Analysis. (preprint).
- Huang, N.E., P.A. Hwang, H. Wang, S.R. Long, and L.F. Bliven, 1983: A study on the spectral models for waves in finite water depths. *J. Geophys. Res.*, 88, 9579-9587.
- Hubert, W.E., 1964: Operational forecasts of sea and swell. *Proc. 1st. U.S. Navy Symp. on Military Oceanography*, 113-124.
- Lighthill, J., 1978: *Waves in Fluids*. Cambridge Univ. Press.
- Peregrine, D.H., 1976: Interaction of water waves and currents. *Advances in Applied Mech.*, 16, 10-117.
- Pierson, W.J., and L. Moskowitz, 1964: A proposed spectral form for fully developed wind seas based on the similarity theory of S.A. Kitaigorodskii. *J. Geophys. Res.*, 69, 5181-5190.
- Phillips, O.M., 1980: *The dynamics of the upper ocean* (2nd. edition). Cambridge Univ. Press.
- Shemdin, O.H., S.V. Hsiao, H.E. Carlson, K. Hasselmann, and K. Schulze, 1980: Mechanisms of wave transformation in finite depth water. *J. Geophys. Res.*, 85, 5012-5018.
- The SWAMP group, 1985: *Ocean wave modeling*. Plenum Press.
- Thornton, E.B., 1977: Rederivation of the saturation range in the frequency spectrum on wind-generated gravity waves. *J. Physical Oceanog.*, 7, 137-140.